UC Irvine
UC Irvine Previously Published Works

Title
Measured signatures of low energy, physical sputtering in the line shape of neutral carbon emission

Permalink
https://escholarship.org/uc/item/5pj1z2gb

Journal
Journal of Nuclear Materials, 337(1-3)

ISSN
0022-3115

Authors
Brooks, NH
Isler, RC
Whyte, DG
et al.

Publication Date
2005-03-01

DOI
10.1016/j.jnucmat.2004.10.058

Copyright Information
This work is made available under the terms of a Creative Commons Attribution License, availalbe at https://creativecommons.org/licenses/by/4.0/

Peer reviewed

eScholarship.org Powered by the California Digital Library
University of California

Available online at www.sciencedirect.com
SCIENCE DIRECT®
Journal of Nuclear Materials 337–339 (2005) 227–231
journal of nuclear materials
www.elsevier.com/locate/jnucmat

Measured signatures of low energy, physical sputtering in the line shape of neutral carbon emission

N.H. Brooks [a,*], R.C. Isler [b], D.G. Whyte [c], M.E. Fenstermacher [d], R.J. Groebner [a], P.C. Stangeby [e], W.W.Heidbrink [f], G.L. Jackson [a], M.A. Mahdavi [a], W.P. West [a], The DIII-D Team

[a] *General Atomics, P.O. Box 85608, San Diego, CA 92186-5608, USA*
[b] *Oak Ridge National Laboratory, Oak Ridge, TN 37831-6169, USA*
[c] *University of Wisconsin, Madison, WI 53706, USA*
[d] *Livermore National Laboratory, Livermore, CA 94550, USA*
[e] *University of Toronto Institute for Aerospace Studies, Toronto, Canada M3H 5T6*
[f] *University of California, Irvine, CA 92697, USA*

Abstract

The most important mechanisms for introducing carbon into the DIII-D divertors [J.L. Luxon, Nucl. Fusion 42 (2002) 614] are physical and chemical sputtering. Previous investigations have indicated that operating conditions where one or the other of these is dominant can be distinguished by using CD and C_2 emissions to infer C I influxes from dissociation of hydrocarbons and comparing to measured C I influxes. The present work extends these results through detailed analysis of the C I spectral line shapes. In general, it is found that the profiles are actually asymmetric and have shifted peaks. These features are interpreted as originating from a combination of an anisotropic velocity distribution from physical sputtering (the Thompson model) and an isotropic distribution from molecular dissociation. The present study utilitzes pure helium plasmas to benchmark C I spectral profiles arising from physical sputtering alone.
© 2004 Elsevier B.V. All rights reserved.

PACS: 52.55.Fa; 52.40.Hf; 52.25.Vy
Keywords: Carbon; Helium; Impurity sources; Spectroscopy; Sputtering

1. Introduction

Most tokamaks operating with high input powers employ graphite tiles for divertor targets and for first walls. As a result of plasma-wall interactions, carbon constitutes the major plasma impurity, so its production mechanisms and transport have been studied extensively. The development of spectroscopic techniques for distinguishing between carbon produced by chemical or by physical sputtering in the DIII-D tokamak has been reported previously [1]. Analysis relies on measurements of C I, CD, and C_2 emissions for evaluating influxes and on determination of effective atomic temperatures [2].

The present work focuses on spectroscopic analysis of C I line shapes in pure helium plasmas, where only

* Corresponding author. Tel.: +1 858 455 3979; fax: +1 858 455 4156.
E-mail address: brooks@fusion.gat.com (N.H. Brooks).

0022-3115/$ - see front matter © 2004 Elsevier B.V. All rights reserved.
doi:10.1016/j.jnucmat.2004.10.058

physical sputtering should contribute to surface erosion. For near-normal viewing onto a divertor target, asymmetries are anticipated from physical sputtering since most of the carbon atoms move toward the observer, in contrast with the symmetric profiles expected from the nearly isotropic velocity distribution for atoms produced from molecular dissociation. Shifts of the profile peaks can result for several reasons, which are discussed in Section 3. In Section 4, the C I line shapes for a density scan in helium plasmas are fit to Thompson velocity distributions and the results interpreted in terms of the energy and charge state of the particles incident on the divertor plate.

2. Apparatus

A schematic drawing of a typical lower single-null (LSN) magnetic configuration in DIII-D is shown in Fig. 1 together with cross-sections of flux surfaces [3]. Seven of the near-vertical views of the absolutely calibrated multichordal divertor spectrometer (MDS) into the lower divertor are also depicted. Five additional sight lines oriented upward into the top of the machine are not shown. Signals are transported through 65 m optical fibers to a 1.3 m Czerny–Turner spectrometer equipped with a 1200 line/mm grating. At the wavelength of the C I line used for the present studies, 9094.829 Å, the dispersion is approximately 0.11 Å/pixel. Twelve fibers from the machine are clamped, together with one short fiber above and another below, into a straight vertical array of fourteen fibers at the entrance slit of the spectrometer. The two outer fibers can be illuminated with various gas discharge lamps to obtain wavelength fiducials, while tokamak data are acquired on the central twelve. For the shot sequences in helium plasmas described in Section 4, the Ar I line at 9122.966 Å has served as the wavelength fiducial, but in the deuterium plasmas discussed in Section 5, where discharge lamp spectra were not recorded, other methods were utilized to evaluate shifts. Information from all channels is recorded simultaneously by a two-dimensional, charge-coupled device (CCD) with 22.5 μ pixels. An integration time of 125 ms is employed. Spectrometer slits are set at 20 μ in order to retain the capability for high-resolution line-profile measurements. Although the input slit is straight, its image at the exit of the spectrometer is curved because of spherical optics, and it is important to account for this aberration accurately when calculating relative shifts between data in different channels. The offset between the end fibers and the center can differ by as much as one pixel, which is more than the actual shift of the peak of the C I line caused by real physical processes under many conditions. The fiber-to-fiber offset caused by this optical distortion is 0.05–0.10 pixel widths or approximately 0.005–0.010 Å.

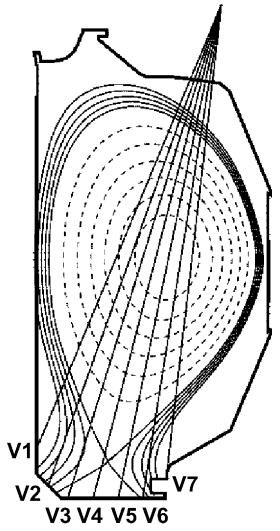

Fig. 1. Schematic view of DIII-D cross-section showing a lower single-null magnetic configuration and views V1–V7 of the multi-chordal divertor spectrometer.

3. Theoretical line shapes

Spectral line shapes from physically sputtered atoms are calculated using a modified Thompson flux distribution of the form [2]

$$f(E)\,\mathrm{d}E = \frac{E}{(E+U_0)^3}\cos^{\alpha}(\theta+\delta)G(E)\,\mathrm{d}E \qquad (1)$$

with $G(E) = 1 - [E + U_0/\gamma(1-\gamma)E_{\mathrm{imp}}]^{1/2}$ and $\gamma = 4m_{\mathrm{D}} \times m_{\mathrm{C}}/(m_{\mathrm{D}} + m_{\mathrm{C}})^2$. E_{imp} is the energy of the incident particles, E is the energy of the sputtered particles, U_0 is the binding energy of carbon (7.4 eV). As indicated in Fig. 2, θ is the angle of the sputtered particle relative to the sight line and δ is the angle between the sight line and

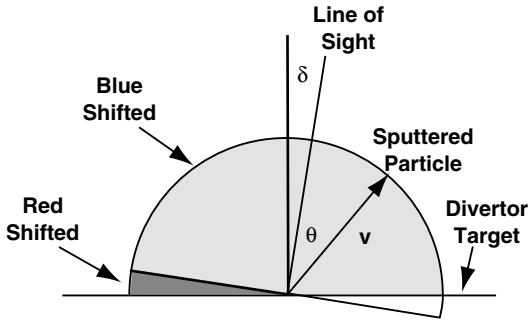

Fig. 2. Velocity space geometry for computing line profiles. Particles in the lightly shaded area contribute to the blue wing; those in the heavily shaded area to the red wing.

the normal to the divertor target. $G(E)$ is a cutoff term that accounts for the maximum momentum that can be transferred to the target atoms. The factor $(1-\gamma)$ is added to Thompson's original term in order to give a better representation for sputtering by light ions [4].

After expressing Eq. (1) in terms of velocities, a distribution in θ and $\Delta\lambda$ is obtained by using the Doppler shift relationship, $\Delta\lambda/\lambda_0 = v\cos\theta/c$. Integration over the angular variables then produces a line profile as a function of $\Delta\lambda$, the wavelength offset from the nominal line center [5]. For a view normal to the target, the resultant profile has only a blue wing since all ejected particles move toward the observer. However, the actual views into DIII-D (Fig. 1) are not normal, and a small fraction of sputtered particles actually moves away from the observer and contributes to a weak red wing. The geometry is illustrated schematically in Fig. 2 where the lightly shaded portion of a semi-circular cross-section in velocity space gives rise to the blue wing. The contribution of atoms in the heavily shaded portion provides the signal near $\Delta\lambda = 0$ in the red wing.

Line shifts as well as line shapes are important for interpreting source mechanisms, but shifts by themselves are difficult to interpret since they can arise for more than one reason. As a consequence of the non-normal views, even a Thompson velocity distribution that is isotropic in θ above the target [$\alpha = 0$ in Eq. (1)], produces a line with a maximum shifted to the low wavelength side of λ_0. Much larger shifts in the line profile maximum should be observed if the angular distribution is strongly peaked normal to the target, even in a normal view. For example, a $\cos\theta$ distribution ($\alpha = 1$) has no atoms moving perpendicular to the sight line, so the intensity is zero at $\Delta\lambda = 0$. Fig. 3 shows calculated profiles for $E_{\mathrm{imp}} = 100\,\mathrm{eV}$ and $\alpha = 1$ for both a normal view and a non-normal one with $\delta = 12°$.

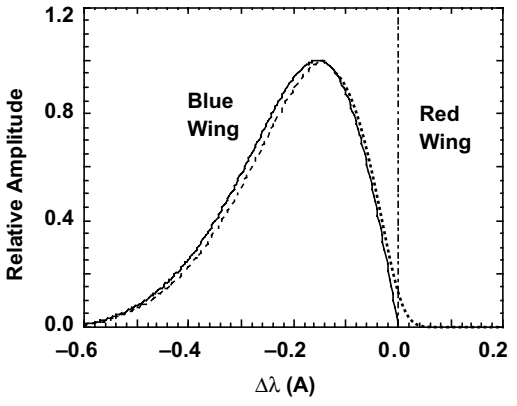

Fig. 3. Calculated spectral profiles from Eq. (1) for viewing along the normal to the divertor target (solid line) and viewing at an angle of 12° (dashed line).

The red-wing contributions from physical sputtering should be small for any of the views onto the DIII-D divertor target. However, the experimental data always exhibit significant emission in the red wing. This emission longward of λ_0 can be reasonably well accounted for by modeling the signal received by the collection lens as a combination of direct and indirect light, the latter caused by reflection from the graphite floors tiles. Because the source region of the indirect light is not identical with that of the direct light for views that are off normal, an effective reflectivity incorporates both the reflectivity of graphite at the C I wavelength as well as any spatial variation in the source function. Reflection has no effect on line shape for a velocity distribution which is isotropic; but, on one which is anisotropic, it causes a reversal of the line profile about the rest wavelength of each Zeeman component. Effective reflectivities between 15% and 20%, which exceed measured reflectivities [6] only slightly, have been found to give good agreement with the measured emission on the red wing of the C I line.

4. C I profiles due to sputtering by helium

All analysis has been performed on the brightest line of the C I ^3P–$^3P^0$ multiplet (9094.826 Å) [1]. To obtain spectral data in which the C I profile was determined solely by physical sputtering under well-documented, steady state conditions, ohmic plasmas were run in pure helium. A rapid switchover from deuterium so helium was achieved by using divertor cryopumping to exhaust residual deuterium from ECH-heated, helium discharges. Neutron analysis and spectroscopy confirmed that a D/He fraction of less than 0.5% was obtained in the highest density ohmic discharges, and approximately 1% as the lowest density.

A shot-by-shot scan in density was performed in ohmic, helium discharges. Fig. 4(a) shows spectra of the Zeeman-split C I line at the outer strike point, taken along view V6. In most cases, the C I line was bright enough for quantitative analysis only at the outer strike point. As density decreases and, concomitantly, the impact energy of helium ions incident on the target increases, the peaks of the π- and σ-components shift to shorter wavelength and their profiles broaden asymmetrically. The overlap of the blue wing of the central π-component with the red wing of the short wavelength σ-component on view V6 necessitates modeling the ensemble of three Zeeman components.

Fig. 4(b) shows the best fit to the data at $\langle n_e\rangle_l = 3.5\times10^{13}\,\mathrm{cm}^{-3}$, of a model profile consisting of a Thompson velocity distribution for physical sputtering convolved with the instrumental profile. The shoulder seen on the right side of each Zeeman-component in the measured profile is due to an indirect (reflected) light

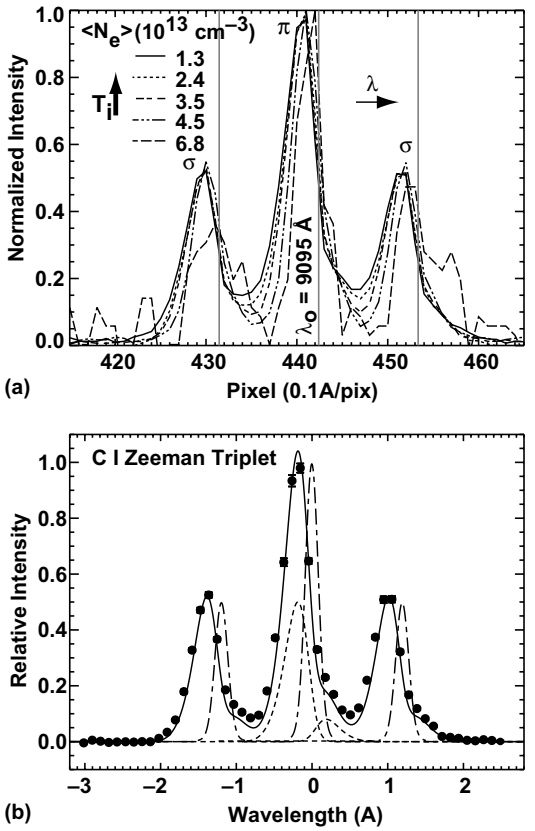

Fig. 4. (a) Peak-normalized profiles of the Zeeman-split C I line in ohmically heated plasmas of pure helium for five different values of line-averaged core density. The positions of the rest wavelengths for the three Zeeman components are indicated by the vertical lines. (b) Fit of theoretical Thompson distribution to measured C I line profile for $\langle n_e \rangle = 3.5 \times 10^{19}\,\mathrm{m}^{-3}$, with instrumental profile shown for comparison. The solid line represents the fit, the solid circles the measured data, the long-short dashed line the instrument profile. The dashed curves left and right of the C I rest wavelength, are, respectively, the predicted Thompson profile for an impact energy of 300 eV and its indirect contribution, mirrored about the rest wavelength and attenuated by the effective reflectivity.

contribution – the reversal on reflection in the apparent direction of the particle motion relative to the observer results in a spectral mirroring of each Zeeman component about its rest wavelength. The direct and indirect contributions to the π-component, respectively, are depicted at half of normalized intensity (for clarity) by the two dashed curves. A good fit to the complex shape of the measured profile is obtained only when the indirect contribution is included in the model spectrum. In the case shown here, the χ^2 fit parameter is minimized for an impact energy of about 300 eV.

The dependence of the electron temperature in front of the divertor target as a function of the line-averaged density in the core plasma, is shown in Fig. 5. These T_e values were obtained from divertor and SOL Thomson scattering measurements during stepwise radial sweeps of the outer strike point – no Langmuir probe data was obtained on this experimental day. Because the SOL electron temperature in these helium discharges exhibited a very shallow gradient between the X-point and the target and there was a paucity of Thomson data immediately in front of the target, all data below the X-point were averaged in the determination of the target T_e and its error bar. Target T_e varies from roughly 10 eV for the highest density discharge to above 30 eV for the lowest density. For the calculation of the E_{imp}/T_e ratio, T_e values are taken from the parabolic fit drawn through the error bars.

At the highest density, the E_{imp}/T_e ratio of roughly five is consistent with acceleration of thermal He^+ ions through a sheath potential of $3kT_e$. The increasing values for E_{impact}/T_e with decreasing density suggest a rising fraction of He^{++} ions incident on the target; for ratios greater than eight, these He^{++} ions must be hotter than the local electron temperature in front of the target. Though simple calculations show that helium ions recycling at the target will re-ionize within a couple centimeters of the plate for the range of temperature and density spanned by these discharges, the result of more comprehensive fluid-edge modeling shows a surprisingly large fraction of He^{++} incident on the OSP, suggestive of alternative pathways by which recycled particles enter the SOL flow to the target. Evidence for He^{++} ions in the SOL with temperatures characteristic of the pedestal region is found in the measurement by charge exchange recombination spectroscopy of ion temperatures and densities in the SOL at the outer midplane. If some of these presumably banana-confined, hot particles scatter into loss orbits, they will significantly enhance sputtering at the divertor target in the low density discharges. Sput-

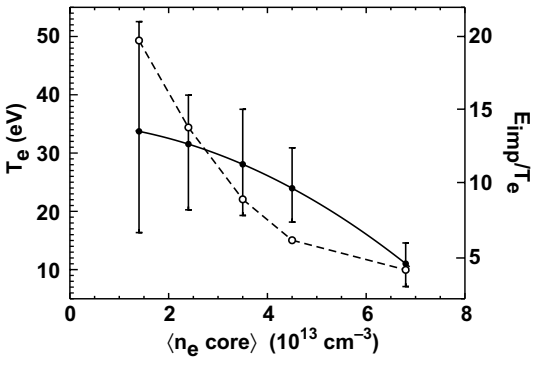

Fig. 5. Comparison of the impact energies inferred from spectral fitting to local T_e in front of the target. Solid circles are result of parabolic fit to mean T_e values; open circles represent E_{imp}/T_e.

tering controlled by fuel particles leaking from the edge plasma onto open field lines upstream of the divertor accords with observations made on JET (the Joint European Torus) [7].

Overall, the Thompson velocity distribution, with inclusion of reflected light in the model, provides a credible match to the subtle details of the measured C I profiles resulting from physical sputtering of carbon by helium at energies of impact in the range 75–500 eV.

5. Summary

Ohmic plasmas in pure helium were produced to study the C I line shape in the presence of physical sputtering alone and, thereby, validate under realistic divertor conditions the Thompson velocity distribution for physical sputtering at low impact energy (75–500 eV). To determine accurately the small Doppler shift anticipated, a very careful wavelength calibration was performed. Inclusion of the wavelength-mirroring effect of indirect observation on line shape was found necessary to achieve a good fit to the red wing of the line. The refinement in line-fitting technique provided by this exercise helps in modeling the more complex line shapes produced in deuterium plasmas, where both physical and chemical sputtering both play a role. In deuterium plasmas, the degree of asymmetry in the C I line shape is found to vary widely with divertor conditions.

Acknowledgment

This work was supported by the US Department of Energy under DE-FC02-04ER54698, DE-AC05-00OR22725, DE-FG03-96ER54373, W-7405-ENG-48, and SC-G903402.

References

[1] R.C. Isler, R.J. Colchin, N.H. Brooks, T.E. Evans, W.P. West, D.G. Whyte, Phys. Plasmas 8 (2001) 4470.
[2] M.W. Thompson, Philos. Mag. 18 (1968) 377.
[3] J.L. Luxon, Nucl. Fusion 42 (2002) 614.
[4] J. Bohdansky, J. Roth, H.L. Bay, J. Appl. Phys. 51 (1980) 2861.
[5] R.C. Isler, R.J. Colchin, N.H. Brooks, T.E. Evans, W.P. West, D.G. Whyte, J. Nucl. Mater. 313–316 (2003) 873.
[6] E.M. Hollmann, A.Yu. Pigarov, R.P. Doerner, Rev. Sci. Instrum. 74 (2003) 3984.
[7] G. Matthews, A. Kallenbach, Bull. Am. Phys. Soc. 45 (2000) 89.